

Analysis of steady state recycling chromatography using equilibrium theory

Tuomo Sainio¹, Malte Kaspereit^{2*}

¹ Lappeenranta University of Technology,
Skinnarilankatu 34, FIN-53850 Lappeenranta, Finland

² Max-Planck-Institut für Dynamik komplexer technischer Systeme,
Sandtorstrasse 1, D-39106 Magdeburg, Germany

Abstract

This paper presents a method for analysis and design of steady state recycling (SSR) chromatography under arbitrary purity or yield requirements. The approach applies to SSR processes in mixed-recycle operation and allows for the direct prediction of the steady state and the design parameters without performing dynamic simulations. Therefore, it simplifies optimal design of SSR processes and evaluation of process performance, while allowing minimizing the startup time of the process.

It was shown that, when the purity and/or yield of the product fractions is specified, the total injection width is the only free operating parameter in mixed recycle SSR chromatography. Theoretical analysis of the process revealed that the productivity is necessarily lower than that of an optimized separation by batch chromatography. On the other hand, the SSR process always outperforms batch chromatography in terms of eluent consumption and product concentrations.

Keywords: chromatography, steady state recycling, equilibrium theory, analysis, optimization

* Corresponding author. Phone: + 49 – 391 – 6110 282, Fax: + 49 – 391 – 6110 551,
Email: kaspereit@mpi-magdeburg.mpg.de (M. Kaspereit)

Nomenclature

Latin letters

A	Coefficient matrix in Eq. (7)
b	Langmuir parameter, $L \text{ mol}^{-1}$, $L \text{ g}^{-1}$
c	Concentration, mol L^{-1} , g L^{-1}
\bar{c}	Average concentration in a product fraction, mol L^{-1} , g L^{-1}
EC	Eluent consumption
m	Mass, kg
P^j	Purity of fraction j with respect to a target component, –
P_i	Plateau in a chromatogram with constant concentration of i
PR	Productivity
q	Stationary phase concentration, mol L^{-1} , g L^{-1}
q_m	Saturation capacity of the adsorbent, mol L^{-1} , g L^{-1}
R	Recycle ratio, –
t	Dimensionless time relative to beginning of cycle, –
u	Interstitial velocity,
V	Injection volume, L
x	Dimensionless space coordinate, –
Y	Yield with respect to a target component, –

Greek letters

Γ	Characteristic of a simple wave
ε	Bed porosity, –
ϕ	Phase ratio, –
ξ	Slope of characteristic in the hodograph plane, –
Σ	Shock wave
τ	Dimensionless time relative to the end of injection, –

Subscripts

1, 2	Components to be separated
A1	Beginning of product fraction A
A2	End of product fraction A
B1	Beginning of product fraction B
B2	End of product fraction B
col	Column
cycle	Cycle of an SSR process
inj	Injection
P	Injection plateau
rec	Recycle fraction
+	Faster wave or shock
–	Slower wave or shock

Superscripts

A	Product fraction A
B	Product fraction B
F	Steady state feed
F0	Fresh feed
P1F	Pure component 1 plateau
T	Transmitted wave

1. Introduction

Chromatography is one of the most important separation techniques in the pharmaceutical and fine chemical industries. Chromatographic techniques are successfully applied to numerous difficult preparative problems such as, for example, the separation of enantiomers [1].

When optimizing preparative chromatographic processes, one can observe a distinct trade-off between performance parameters. For example, an unconstrained maximization of throughput leads to very high injection volumes, which entail large portions of the chromatogram to be remained unresolved. Discarding the latter is barely acceptable in the case of expensive substances.

In the case of binary separations, Simulated Moving Bed (SMB) chromatography is an option to circumvent this problem, since this process has no waste stream. However, besides SMB systems, which suffer from rather high investment costs, several interesting single-column techniques have been suggested that enhance the yield by recycling the chromatogram partially or as a whole. In closed-loop recycling [2–4], the whole elution profile is recycled several times over the same column until complete separation is achieved. Back mixing that occurs in the recycle pump can be averted (at the expense of higher eluent consumption) by sophisticated column or pump arrangements (e.g., “alternate pumping” [5]). Further improvement is achieved by so-called peak shaving (see, e.g. [3]), wherein the pure leading and trailing sections of the chromatogram are collected (“shaved”), while only the unresolved remainder is recycled. Steady state recycling (SSR) chromatography is a further development of the above concepts. In SSR processes, in addition to collecting the purified leading and trailing parts of the elution profile, a constant amount of fresh feed is added to each recycle fraction, which causes the process to attain a periodic steady state.

Different operating modes were proposed for SSR chromatography. In “mixed-recycle” mode [6], the whole recycle fraction is first collected and mixed with fresh feed before re-injection. Based on the equilibrium theory, an approach for analysis and design of this process was devised for the case of complete separation [6–9]. Using numerical simulations, it was shown that the mixed-recycle mode allows a reduction of eluent consumption also for systems with limited efficiency and, under certain conditions, enhancement of productivity [10].

Another SSR operating policy, the “closed-loop” mode [11], has gained considerable attraction. In order to preserve the already achieved partial separation of the recycle fraction, closed-loop recycling is combined with the injection of (unmixed) fresh feed. This concept appears particularly useful for very difficult separations and its feasibility has been demonstrated in several experimental studies [11–15]. Besides this, also other modes were proposed; for example, “segmented recycling” (i.e., injection of the mixed recycle fraction before the fresh feed) and “combination of recyclings” (re-injection of the dispersed tail of the stronger adsorbing component, followed by the recycle fraction and, finally, fresh feed) [9, 10].

Although closed-loop SSR chromatography is (apparently in contrast to the mixed-recycle option) successfully commercialized by the company Novasep (Pompey, France), so far only an empirical experimental design method exists for this process (see, e.g., [11]). Unfortunately, the procedure neither allows the *a priori* estimation of the steady state, nor does it guarantee the fulfillment of purity requirements or optimum performance. The mentioned equilibrium analysis for SSR processes with mixed-recycle (e.g., [6, 9]) meets these criteria, but suffers from a certain complexity. Finally, both design approaches hold only for two pure product fractions.

In view of the above aspects, the main goal of this work is to provide a theoretical framework that allows i) for a straightforward analysis and optimal design of SSR chromatography, and ii) to apply SSR processes to separation problems with arbitrary purity requirements. For this purpose, we will extend the application range of equilibrium theory to mixed-recycle SSR processes under arbitrary purity requirements.

This contribution is structured as follows. After a short summary of the main principles of SSR chromatography, the theoretical framework will be developed. It will be shown that the steady state of an SSR process can be predicted directly from the adsorption isotherms and the composition of the fresh feed, which largely simplifies process analysis and optimal design. Subsequently, the method will be used to assess the performance of SSR chromatography with mixed-recycle for a generic example with competitive Langmuir adsorption isotherms. As will be shown, the approach is a useful tool for evaluation and design of process performance, since it predicts the optimum performance of an SSR process and allows to minimize the startup time of the process. Finally, a short discussion will be given on practical aspects and the applicability of the method to design mixed-recycle SSR processes.

2. Principle of SSR chromatography

The principle of SSR chromatography and different technological options for its practical realization have been described in detail elsewhere (e.g., [10–12]). Here we will explain only the most fundamental aspects.

Figure 1 (top) contains a scheme of an SSR process. Depending on the operating mode (i.e., mixed-recycle or closed-loop SSR), one or more pumps and several multi-port valves are required to realize the alternating streams of fresh feed mixture (F0), eluent (E), and recycle (R), and the collection of the product fractions A and B, respectively.

There are several options to initiate an SSR process. The commonly used approach results in concentration profiles as shown in Fig. 1 (bottom). The process is started by injecting a small amount of fresh feed mixture (F0) onto the initially unloaded column. The actual SSR cycle starts at time t_{A1} , when the column effluent is directed to fraction A to collect the less adsorbed component 1 (solid lines). Between t_{A2} and t_{B1} the recycle fraction elutes, which contains both species. In mixed-recycle mode, the whole recycle fraction is collected in a

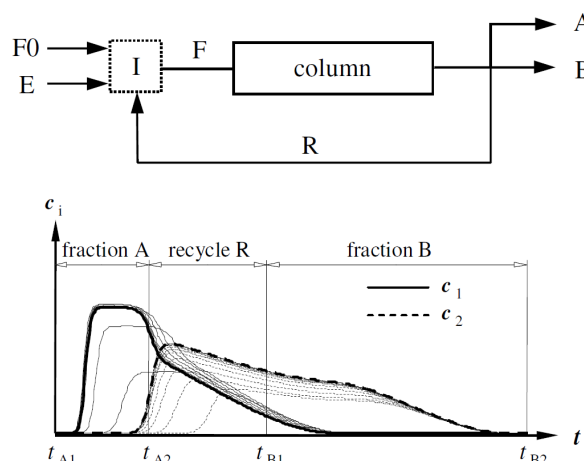


Figure 1. Top – Schematic representation of an SSR process. F0, fresh feed; F, column feed; E, eluent; A, product fraction (weaker adsorbing component 1); B, product fraction (strong adsorbing component 2); R, recycle fraction; I, injection port (injection loop in closed-loop mode, or mixer in mixed-recycle mode). Bottom – Example for fraction collection and startup behavior in mixed-recycle mode. The diagram shows an overlay of the concentration profiles at column outlet for cycles 1, 3, ..., 25. Thick lines: concentration profiles at steady state (cycle 25). The cut times are relative to the start of the corresponding injection.

reservoir, mixed with fresh feed and then injected. In closed-loop recycling mode, the outlet is now connected to the column inlet; fresh feed is injected again at a certain position during this step by switching an injection loop into the recycle stream. In both modes, after time t_{B1} , fraction B (containing an excess of component 2, dashed lines) is collected until the chromatogram is eluted completely at t_{B2} .

By repeating the above procedure several times, the two components accumulate in the system until a periodic steady state is attained in which the chromatograms and the average product compositions do not vary from cycle to cycle. This is shown in the bottom of Fig. 1. Please note that in the example four cut times (t_{A1} , t_{A2} , t_{B1} , t_{B2}) were chosen such that two product fractions are obtained with purities below 100%. Such cases are in the scope of this work.

It should be emphasized that a systematic comparison of the performance of closed-loop and mixed-recycle SSR processes is beyond the scope of this work. However, the mixed-recycle mode has – besides the disadvantage of “destroying” the already partially resolved concentration profile of the recycle – also some distinct advantages and can outperform batch chromatography [10]. Therefore, a brief discussion of relevant aspects will be given in section 5.

A significant problem related to SSR chromatography is that an optimal design is difficult due the dynamic character of the process. Obviously, given the purity requirements as constraints, the main design parameters are the injection volume and the cut times. However, the optimal values for these parameters depend on the steady state concentration profiles and *vice versa*. As already mentioned, the only existing design approach for the closed-loop operating mode is an empirical shortcut method based on an experimental procedure [11]. Although the method

is thoughtful and simple to apply even with only little knowledge of system properties, its drawback is that it gives no prediction with respect to the steady state and process performance. These are accessible only by actually carrying out an SSR process until steady state is obtained. Furthermore, the approach does not guarantee the intended complete separation or optimal process performance. For the mixed-recycle mode, on the other hand, an equilibrium-design approach [6, 9] is available for the limiting case of 100 % purity and yield.

Another important aspect is the startup behavior (cf. Fig. 1, bottom). Process performance (i.e., product concentrations, productivity, and eluent consumption) is limited during this startup phase and – depending on the operating parameters – a rather large number of cycles can be required to attain steady state. Approximately 20 cycles seem to be necessary [11–13]. However, if the steady state (i.e., the recycle composition and volume) is known, the duration of the startup could be minimized to only a single cycle by initiating the process with a “full injection” (i.e., volume of recycle plus fresh feed) with steady state concentrations [6].

As will be shown in the next section, analyzing the mixed-recycle SSR operation in the frame of equilibrium theory allows for a direct prediction of the steady state for corresponding SSR processes with arbitrary purity requirements and, thus, to tackle some of the shortcomings of the existing design approaches.

3. Theory of SSR chromatography

As usual in designing separation processes, the goal is to find operating parameters that lead to optimal process performance. In the present case, these are the four cut times (t_{A1} , t_{A2} , t_{B1} , and t_{B2}) shown in Fig. 1 and the injection width (Δt_{inj}). Here we present a method for choosing the operating parameters such that, in the steady state, arbitrary purity and/or yield constraints can be satisfied. For this purpose we will adopt the so-called equilibrium theory of chromatography for systems that follow the competitive Langmuir adsorption model. The approach is similar to that chosen by Bailly, Tondeur, and Charton [6, 9], but will be extended here to the case of arbitrary purity and yield requirements.

As will be shown below, it is possible to determine three of the four cut times directly from the isotherm parameters, without carrying out a dynamic column simulation from the initial state of the system to the steady state. In fact, these three cut times (i.e., t_{A2} , t_{B1} , and t_{B2} in Fig. 1) are sufficient to fully determine the steady state feed concentrations. The fourth cut time (t_{A1}) is required only to assess process performance. Under certain conditions, also t_{A1} can be determined explicitly; otherwise a single integration of a steady-state chromatogram is required.

3.1 Design specifications

In this work, it is assumed that the desired purities of the product fractions are known as design constraints. With respect to Fig. 1, these are given by

$$P^A = \frac{m_1^A}{m_1^A + m_2^A} = \int_{t_{A1}}^{t_{A2}} \frac{c_1}{c_1 + c_2} dt \quad (1)$$

$$P^B = \frac{m_2^B}{m_1^B + m_2^B} = \int_{t_{B1}}^{t_{B2}} \frac{c_2}{c_1 + c_2} dt \quad (2)$$

where m_i^j denotes the mass of component $i=(1, 2)$ in product fraction $j=(A, B)$. As an alternative to the specifications of desired purities, the yields of the components in the desired product fractions can be given. These are defined as follows

$$Y_1 = \frac{m_1^A}{m_1^{F0}} = \frac{\int_{t_{A1}}^{t_{A2}} c_1 dt}{c_1^{F0} [\Delta t_{inj} - (t_{B1} - t_{A2})]} \quad (3)$$

$$Y_2 = \frac{m_2^B}{m_2^{F0}} = \frac{\int_{t_{B1}}^{t_{B2}} c_2 dt}{c_2^{F0} [\Delta t_{inj} - (t_{B1} - t_{A2})]} \quad (4)$$

where the dimensionless injection width $\Delta t_{inj} = (V_{fresh} - V_{rec}) / \varepsilon V_{col}$ refers to the width of the pulse that is fed into the column after mixing the recycle fraction and the fresh feed.

It should be noted that, since the SSR process represents a binary separation without a waste stream, the purity and yield constraints in Eqs. (1) – (4) are interchangeable [16, 17]. From global mass balances around such a process the following relations between the purities and the yields can be derived

$$Y_1 = \frac{P^A}{P^{F0}} \frac{P^{F0} + P^B - 1}{P^A + P^B - 1} \quad (5)$$

$$Y_2 = \frac{P^B}{1 - P^{F0}} \frac{P^A - P^{F0}}{P^A + P^B - 1} \quad (6)$$

where P^{F0} is defined as $P^{F0} = c_1^{F0} / (c_1^{F0} + c_2^{F0})$. In other words, by specifying any two of the four quantities, the remaining two are also determined. In principle, any combination of constraints could be used to determine the cut times and the resulting steady state feed concentrations of the SSR process. However, the most convenient calculation method is obtained by choosing P^B and Y_2 , which will be applied below.

3.2 Hodograph representation of mixed-recycle SSR processes

From a mathematical modeling point of view, operation of a chromatography column in SSR mode does not introduce new phenomena into the calculation domain since fractionation of the effluent stream and mixing of the recycle are performed outside the column. Therefore, in the limit of infinite column efficiency, the conventional ideal model of chromatography, given by Eqs. (7) and (8), can be used to describe the propagation of the concentration states in the column.

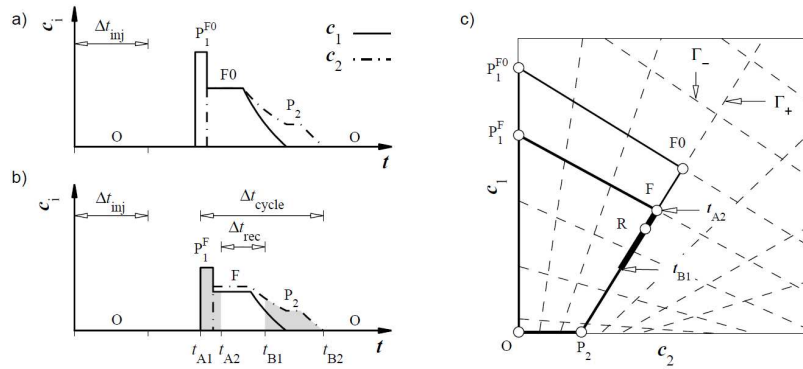


Figure 2. Steady state recycling chromatography in mixed-recycle operation. a) Chromatogram for first injection (injection of fresh feed, concentrations c_i^{F0}). b) Chromatogram at steady state (injection concentrations c_i^F). c) Corresponding hodograph representations.

$$A \frac{\partial \mathbf{c}}{\partial t} + \frac{\partial \mathbf{c}}{\partial x} = 0 \quad (7)$$

where

$$A = \begin{bmatrix} 1 + \phi \frac{\partial q_1}{\partial c_1} & \phi \frac{\partial q_1}{\partial c_2} \\ \phi \frac{\partial q_2}{\partial c_1} & 1 + \phi \frac{\partial q_2}{\partial c_2} \end{bmatrix}, \quad \mathbf{c} = \begin{bmatrix} c_1 \\ c_2 \end{bmatrix} \quad (8)$$

and q is stationary phase concentration, ϕ is phase ratio, x is a reduced space coordinate (at column outlet, $x=1$), and t is a reduced time (elution time of a non-retained component is $t = 1$).

The following discussion is limited to binary systems with adsorption according to competitive Langmuir adsorption isotherms given by

$$q_i = \frac{q_{m,i} b_i c_i}{1 + b_1 c_1 + b_2 c_2}, \quad i = 1, 2 \quad (9)$$

For this isotherm model, Eq. (7) has no analytical solution when the space coordinate, x , and time, t , are the independent variables. However, if the concentrations c_1 and c_2 are used as the independent variables, the model forms a coupled system of two linear first-order partial differential equations, which can be solved analytically by the *method of characteristics*. This is the basis of the so-called equilibrium theory, which we now apply to SSR chromatography. Equilibrium theory is described extensively in the literature [18–20], and only the most relevant aspects can be covered here.

The solutions of Eq. (7) can be constructed in the so-called hodograph plane spanned by the concentrations c_1 and c_2 . An example is given in Fig. 2c. Regions of the solution where the independent variables c_1 and c_2 are functionally related are called *simple waves*. For Langmuir isotherms, simple waves correspond to segments on straight lines, called *characteristics* (dashed lines in Fig. 2c). Characteristics running from the lower left to the upper right are referred to as Γ_+ characteristics, those directed from upper left to lower right as Γ_- characteristics, respectively. Their slopes dc_1/dc_2 can be calculated explicitly

from the right eigenvectors of the coefficient matrix A in Eq. (8), and therefore depend on the isotherm parameters only.

Two distinct propagation velocities are associated with each state (c_1, c_2) , because it can be a part of the solution on either a Γ_+ or a Γ_- characteristic. These velocities can be obtained from the eigenvalues of A . Regions of the solution where c_1 and c_2 are constant are represented by single points on the hodograph plane.

It is well known that the nonlinear nature of Eq. (7) can give rise to discontinuities (such as shock waves) in the solution. In the case of Langmuir isotherms, the images of such discontinuities on the hodograph plane also fall onto the characteristics. Often, the corresponding shock paths are called Σ_+ and Σ_- shocks, respectively. The propagation velocities of shock waves are given by the mass balance across the discontinuity.

Let us recall that a pulse injection into a chromatographic column consists of two step-wise changes of the inlet concentrations. The first step changes the input concentration from the initial state (i.e., pure eluent) to the injection mixture. In the second step (at the end of the injection), the input composition is changed back to the initial state. The network of characteristics in the hodograph plane can be seen to determine the “legal solution path” for the response of the chromatographic column to such step-wise change, because the initial and final states must be connected by the characteristics. For example, let us assume that the chromatogram in Fig. 2a corresponds to a wide pulse of fresh feed with concentrations c_i^{F0} . The corresponding hodograph plot in Fig. 2c shows that the shocks in the front of the elution profile connect the initial state O and the injection plateau $F0$ by segments $O-P_1^{F0}$ and $P_1^{F0}-F0$.

The mixed simple wave eluted after the injection plateau maps on the line segment $F0-P_2$, whereas the pure component 2 wave maps onto the portion $O-P_2$ of the abscissa. Each of the plateaus in the elution profile represents a single point in the hodograph plane, marked with the corresponding letters. The actual route between initial state O and “final” state $F0$ is fixed unambiguously, since the initial state always lies on a Γ_+ characteristic and the final state on a Γ_- characteristic [18, 19].

It is emphasized that for Langmuir isotherms, explicit equations exist for calculating the slopes of the characteristics, their

intersection points, as well as the propagation velocities associated with each concentration state (see, e.g., [18–21]). The only information needed is the isotherm parameters, phase ratio, and the initial and final concentrations.

With respect to SSR chromatography, the question now arises, where would the steady state feed concentration be located in the hodograph plane if the process is carried out by mixing the recycle fraction and fresh feed? Let us assume that the process is started with a wide pulse of fresh feed (F0), resulting in the chromatogram in Fig. 2a and the corresponding hodograph plot (O–P₁^{F0}–F0–P₂–O) in Fig. 2c. The concentration state eluted at cut time t_{B1} during the first injection lies on the segment F0–P₂ for any feasible purity constraint P^B . This is because the concentrations at the rear of the profile cannot exceed F0, and placing the cut position on line segment P₂–O would mean that some pure product is lost since only part of the pure component 2 profile is collected in product fraction B. Also the concentration state eluted at t_{A2} must lie on the line segment F0–P₂ because the cut position is located either on the mixed wave or, in the case of large injection width and high P^A , on the injection plateau. As a consequence, the entire recycle fraction (bold line in Fig. 2c) must map on a segment of the Γ_+ characteristic passing through the fresh feed composition F0. The volume-averaged composition of the recycle is, therefore, represented by a single point (R) within the same line segment. The important consequence of this is that, according to the lever rule, also the composition of the next injection (with results from mixing the fresh feed, F0, with the recycle R), must map to a point on the same Γ_+ characteristic.

In other words, the feed composition cannot move away from the Γ_+ characteristic that passes through (c_1^{F0} , c_2^{F0}) during the subsequent cycles. Eventually, a steady state is reached with feed composition F in the hodograph plot. The corresponding chromatogram is displayed in the bottom of Fig. 2b.

It is clear that, as long as the SSR process is operated such that the purity and yield constraints can be fulfilled, the image of the rear part of the elution profile in the hodograph plane, and thus also in the chromatogram, remains unaltered. This valuable information provides the basis for determining the cut times that fulfill arbitrary purity requirements in steady state. Bailly and Tondeur [6] applied the same principle to determine cut times in the limiting case of 100 % purity of both product fractions. It should be noted, however, the method that we present below for choosing the cut times is not limited to pure products and complete yield.

3.3 Determination of cut times t_{A2} , t_{B1} , and t_{B2}

Since the rear of the profile remains unaltered, we start by determining cut times t_{B1} and t_{B2} . Evidently, the cut time t_{B2} should be chosen such that it matches the time of complete elution of the injection (cf. Fig 2b). It is thus obtained by setting $c_1 = c_2 = 0$ and calculating the eigenvalue of **A** corresponding to the Γ_- simple wave on the abscissa. For Langmuir isotherms, the resulting well known expression for t_{B2} is

$$t_{B2} = \Delta t_{inj} + 1 + \phi \left. \frac{dq_2}{dc_2} \right|_{\substack{c_1=0 \\ c_2=0}} = \Delta t_{inj} + 1 + \phi q_{m,2} b_2 \quad (10)$$

As a next step, cut time t_{B1} is chosen such that the purity constraint of product fraction B, Eq. (2), is fulfilled. Although an explicit expression for t_{B1} can be obtained, it is rather complex and it was found more convenient to use a fast numerical technique: while using a search algorithm to find the lower integration limit that satisfies Eq. (2), the integral terms in this equation are evaluated analytically. The required analytical expressions for $c_i(t)$ are given, for example, by Guiochon et al. [21]

As noted earlier, purity constraints can equivalently be given as yield constraints. Once t_{B2} is obtained, the yield constraint of component 2, displayed in Eq. (4), can be solved for t_{A2}

$$t_{A2} = t_{B1} - \Delta t_{inj} + \frac{\int_{t_{B1}}^{t_{B2}} c_2 dt}{c_2^{F0} Y_2} \quad (11)$$

As seen in the equation, the beginning and end of the recycle fraction can be determined without knowing the steady state feed concentration.

It is also interesting to note that the cut time t_{A2} is independent of the injection width. This is observed by rewriting Eq. (11) in terms of the elution time relative to the end of the injection, $\tau = t - \Delta t_{inj}$, as follows

$$t_{A2} = \tau_{B1} + \frac{\int_{\tau_{B1}}^{\tau_{B2}} c_2 d\tau}{c_2^{F0} Y_2} \quad (12)$$

Since this transformation is merely a linear shift on the abscissa, the value of the integral term remains unaffected. Applying the same transformation to Eq. (2) shows that also τ_{B1} is independent of injection width.

3.4 Determination of steady state feed composition

The steady state feed concentration, c_1^F , corresponding to a given injection width can be calculated from the following mass balance of component 1 around the feed node

$$c_1^F \Delta t_{inj} = \int_{t_{A2}}^{t_{B1}} c_1 dt + c_1^{F0} [\Delta t_{inj} - (t_{B1} - t_{A2})] \quad (13)$$

A functional relationship between c_1^F and c_2^F is given by the slope ξ_+^{F0} of the Γ_+ characteristic that passes through F0 (see Fig. 2c), which depends on the isotherm parameters and the fresh feed composition. Thus, for c_2^F holds:

$$c_2^F = c_2^{F0} + \frac{1}{\xi_+^{F0}} (c_1^F - c_1^{F0}) \quad (14)$$

It is interesting to note that the steady state feed composition becomes independent of Δt_{inj} when t_{A2} is located on the injection

plateau (*i.e.*, for large injection volumes). This is observed by rewriting Eq. (13) as

$$c_1^F \Delta t_{inj} = (\Delta t_{inj} + \tau_p - t_{A2}) c_1^F + \int_{\tau_p}^{\tau_{B1}} c_1 d\tau + \dots \quad (15)$$

$$+ c_1^{F0} \left[\Delta t_{inj} - (\Delta t_{inj} + \tau_{B1} - t_{A2}) \right]$$

which can be re-arranged to give

$$c_1^F = \frac{\int_{\tau_p}^{\tau_{B1}} c_1 d\tau + c_1^{F0} (t_{A2} - \tau_{B1})}{t_{A2} - \tau_p} \quad (16)$$

Here τ_p denotes the elution time of the end of the injection plateau relative to the end of the injection and thus depends on c_1^F and the isotherm parameters only. Since t_{A2} and τ_{B1} are also independent of Δt_{inj} , so is the steady state feed concentration.

3.5 Determination of t_{A1}

So far, we have considered only the rear part of the elution profile, which proved to be sufficient to determine the steady state feed concentrations and three of the four cut times. The remaining cut time, t_{A1} , should obviously be chosen equal to the elution time of the pure component 1 shock (cf. Fig. 2b) to minimize the cycle time. The task is therefore to evaluate the elution time of the front shock that corresponds to the steady state feed concentration.

According to the equilibrium theory, the propagation velocity of a shock depends on its height. In the case of a *large injection* width, such as depicted in Fig. 2b, the plateau P_1^F in the front of the elution profile is not eroded during elution. The velocity of the shock is thus constant, and the cut time t_{A1} can be calculated analytically by using Eq. (17)

$$t_{A1} = 1 + \phi \frac{q_1(c_1^{PIF}, 0)}{c_1^{PIF}} \quad (17)$$

where the height of the plateau $c_1^{PIF} = c_1^F - \xi_-^F c_2^F$, is obtained from the slope ξ_-^F of the Γ_- characteristic passing through the steady state feed on the hodograph plane (point F in Fig. 2c).

A typical chromatogram obtained for *small injection* widths is displayed in Fig. 3a. As seen in the figure, for sufficiently small injections, the pure component 1 plateau erodes completely, and the height of the shock decreases while it propagates through the column. In this case, the velocity of the shock is not constant, and a closed-form solution for t_{A1} cannot be found. Several approaches have been applied in the literature for solving this problem. Guiochon et al. [21] describe a calculation method that combines an analytical solution for the rear part of the chromatogram with a numerical scheme for calculating the front of the chromatogram. Rhee et al. [19] present a step-by-step procedure for solving Eq. (7) by tracking the trajectories of the shocks and simple waves in a distance–time plane. The method applied in this work is adapted from that of Rhee et al. For the sake of brevity, only the necessary steps to determine t_{A1} , instead of constructing the entire chromatogram, are described below.

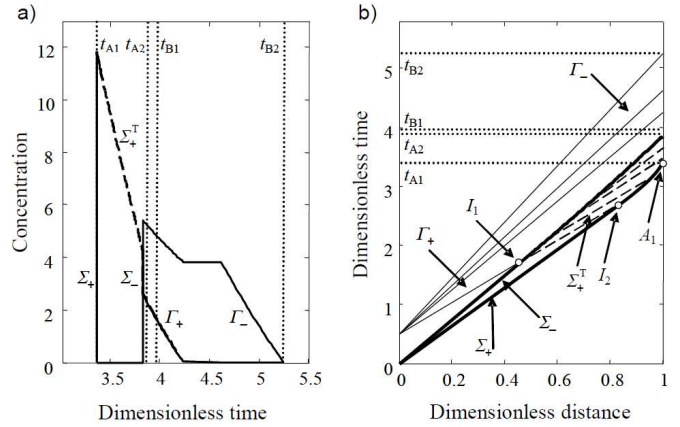


Figure 3. Determination of t_{A1} by integration of Eq. (7) in the t - x plane. a) Typical chromatogram for the case of small Δt_{inj} (wave interaction). b) Trajectories of the shocks and simple waves in t - x plane. Thick lines: shock waves; thin lines: boundaries of simple waves; dashed line: transmitted Γ_+^T wave.

The distance–time diagram representation of a chromatogram corresponding to small injection is displayed in Fig. 3b. The slopes of the shocks (thick solid lines) and simple wave boundaries (thin solid lines) are inversely proportional to their velocities in the column. In order to determine t_{A1} , the location of the point A_1 , where the first shock (Σ_+) reaches the outlet of the column, has to be found.

The two shocks in the front of the elution profile propagate with constant velocities as long as the shock heights are constant. They are, thus, represented by straight lines from the origin until points I_1 and I_2 in the diagram, where interaction of waves starts. These two points are easily mapped on the x - τ plane because the slopes of the intersecting lines are explicitly given by the isotherm data and the steady state feed concentration. The propagation directions of the shocks are obtained from the so-called jump condition as shown in Eq. (18), and the slopes of the simple wave boundaries are obtained from the eigenvalues of the coefficient matrix A in Eq. (8).

$$\frac{d\tau}{dx} \Big|_{\Sigma_+} = 1 + \Phi \frac{q_1^{PIF}(c_1^{PIF}, 0)}{c_1^{PIF}}, \quad (18)$$

$$\frac{d\tau}{dx} \Big|_{\Sigma_-} = 1 + \Phi \frac{q_2^{PIF}(c_1^F, c_2^F)}{c_2^F}$$

At I_1 , the injection plateau vanishes because the mixture wave (Γ_+) reaches the mixture shock (Σ_-). The result of the subsequent wave interaction is a transmitted Γ_+ wave, which contains only component 1. This new wave is indicated with dashed lines in both the chromatogram and the distance–time diagram in Fig. 3 and denoted by Γ_+^T .

As seen in the diagram, the pure component 1 shock travels with a constant velocity until point I_2 , where it begins to interact with the transmitted Γ_+^T wave. During the interaction, the height of the shock decreases, and its propagation velocity is thus reduced. This is observed as a curved trajectory I_2 - A_1 of the shock in the figure. For simplicity, a numerical scheme was used to track this trajectory. It is known that everywhere between I_2 and A_1 , the

height of the Σ_+ shock matches the concentration c_1 on the Γ_+ wave. Therefore, the Γ_+ wave that results from interaction between the Σ shock and the Γ_+ wave was stored as a tabulated function. Starting from I_2 , a small step in the direction determined by the velocity of the Σ_+ shock was taken. The height of the shock at this new point was obtained by numerically solving for the concentration c_1 that is found on the Γ_+ wave at this point. The direction of the Σ_+ shock was updated, and the procedure was repeated until arriving at A_1 (i.e., until $x = 1$).

3.6 Possible extensions of the theory

The above discussion was limited to binary systems with competitive Langmuir adsorption isotherms. However, the method presented here can be applied equally well to multicomponent mixtures when cut times t_{A2} and t_{B1} are located on the first mixed simple wave (where none of the concentrations is zero). In other cases, the steady state feed concentration moves away from the Γ_+ characteristic passing through the fresh feed point in the multidimensional hodograph space, and the cut time t_{A2} cannot be determined by integration of the profiles from the rear.

Further, it is well known that ion exchange equilibria with constant selectivities can be treated analogously to Langmuirian systems [23]. A ternary system reduces to a binary system when the compositions are expressed in equivalent fractions. In fact, the original work on SSR chromatography by Bailly and Tondeur [6] considered ion exchange in the system $H^+/Na^+/K^+$.

4. Performance evaluation of mixed-recycle SSR chromatography

The most common performance parameters of chromatographic processes are the productivity, PR , and eluent consumption, EC . In addition, the average product concentrations, \bar{c}_1^A and \bar{c}_2^B are of interest. The yields, Y_1 and Y_2 , could also be interpreted as performance parameters, but are treated here as constraints because they are interchangeable with P^A and P^B (see Eqs. (5) and (6)).

Eluent consumption and productivity are here defined for component 1 as follows (and analogously for component 2):

$$EC_1 = \frac{\Delta t_{\text{cycle}} - \Delta t_{\text{rec}}}{m_1^A} = \frac{\Delta t_{\text{cycle}} - \Delta t_{\text{rec}}}{Y_1 c_1^{F0} (\Delta t_{\text{inj}} - \Delta t_{\text{rec}})} \quad (19)$$

$$PR_1 = \frac{m_1^A}{\Delta t_{\text{cycle}}} = \frac{Y_1 c_1^{F0} (\Delta t_{\text{inj}} - \Delta t_{\text{rec}})}{\Delta t_{\text{cycle}}} \quad (20)$$

The average concentrations in the product fractions A and B are obtained by integration of the elution profiles with the determined cut times as limits

$$\bar{c}_1^A = \frac{1}{t_{A2} - t_{A1}} \int_{t_{A1}}^{t_{A2}} c_1 dt, \quad (21)$$

$$\bar{c}_2^B = \frac{1}{t_{B2} - t_{B1}} \int_{t_{B1}}^{t_{B2}} c_2 dt$$

It was shown above, that for given purity or yield constraints and a given fresh feed composition, the *injection width is the only freely adjustable operating parameter*. Therefore, we first introduce the explicit dependency of the operational parameters (i.e., the times required for recycling and complete cycle) on the injection width. This has not been attempted in previous works on SSR processes. This allows analyzing its influence on the performance parameters (productivity, eluent consumption, and product concentrations). It should be noted again that the term “injection width” refers to the volume of the pulse obtained by mixing together the recycle fraction and the fresh feed relative to the volume of the column.

To predict the optimum performance of the SSR process, we assume that “stacked injections” can be accomplished. This means that injection times are chosen such that no gap exists between fraction B of the n-th cycle and fraction A of (n+1)-th cycle, (which is possible in mixed-recycle mode). In this case the cycle time is

$$\Delta t_{\text{cycle}} = t_{B2} - t_{A1} = \Delta t_{\text{inj}} + \tau_{B2} - t_{A1} \quad (22)$$

In practice, a safety gap might be desired between the cycles. In such cases the cycle time can be increased accordingly. Overlaps between cycles are not considered here.

The width of the recycle fraction, $\Delta t_{\text{rec}} = t_{B1} - t_{A2}$, increases linearly with increasing Δt_{inj} , as is observed by rearranging Eq. (11) and differentiating with respect to the injection width

$$\frac{\partial \Delta t_{\text{rec}}}{\partial \Delta t_{\text{inj}}} = \frac{\partial (t_{B1} - t_{A2})}{\partial \Delta t_{\text{inj}}} = 1 \quad (23)$$

Using this information, it is found that the amount of fresh feed introduced to the process during each cycle, and consequently the amount of products obtained in steady state, is independent of injection width

$$\frac{\partial m_1^{F0}}{\partial \Delta t_{\text{inj}}} = c_1^{F0} \frac{\partial (\Delta t_{\text{inj}} - t_{\text{rec}})}{\partial \Delta t_{\text{inj}}} = 0 \quad (24)$$

This result means that, in an SSR process, the specification of desired yields or purity requirements fixes the achievable throughput per cycle, which cannot be altered by changing the injection width.

As discussed earlier, the elution time of the pure component 1 shock, t_{A1} , depends on its height. As long as the plateau P_1^F (see Fig. 2b) has not completely eroded, the height of the shock depends on c_1^F only, which was above shown to be constant for large injections. In this case, one obtains from Eqs. (10) and (22) that the cycle time is directly proportional to the injection width (since τ_{B2} is independent of Δt_{inj})

$$\frac{\partial t_{\text{cycle}}}{\partial \Delta t_{\text{inj}}} = \frac{\partial}{\partial \Delta t_{\text{inj}}} (\tau_{B2} + \Delta t_{\text{inj}} - t_{A1}) = 1 \quad (\text{large } \Delta t_{\text{inj}}) \quad (25)$$

In case of small injections, on the other hand, no closed form expression for t_{A1} can be given. A parametric analysis using the approach described in section 3.5, and applying small and large separation factors, low and high purities, as well as weakly and strongly non-linear adsorption isotherms indicated that, in a mixed-recycle SSR process, t_{A1} always increases with Δt_{inj} . Moreover, the derivative $\partial t_{A1} / \partial \Delta t_{\text{inj}}$ was found to be positive but less than unity in all cases. Therefore, we propose the following empirical inequality for the present analysis

$$0 < \frac{\partial t_{\text{cycle}}}{\partial \Delta t_{\text{inj}}} = 1 - \frac{\partial t_{A1}}{\partial \Delta t_{\text{inj}}} \leq 1 \quad (26)$$

4.1 Effect of injection width on performance parameters

Using Eqs. (23) – (26) together with the definition of eluent consumption yields Eq. (27), which states that the eluent consumption decreases monotonically or remains constant with increasing injection width.

$$\frac{\partial EC_1}{\partial \Delta t_{\text{inj}}} = \frac{1}{Y_1 m_1^{F0}} \left(\frac{\partial t_{\text{cycle}}}{\partial \Delta t_{\text{inj}}} - 1 \right) \leq 0 \quad (27)$$

The equality sign refers to large injections where the pure component 1 plateau has not eroded. In other words, increasing the injection width Δt_{inj} improves the performance in terms of eluent consumption. The same result is obtained if the analysis is carried out for component 2.

For productivity, PR_1 , a similar treatment as above yields Eq. (28). Accepting the empirical inequality in Eq. (26) implies that the productivity of mixed-recycle SSR processes always decreases with increasing injection width, which is in accordance with our observations.

$$\frac{\partial PR_1}{\partial \Delta t_{\text{inj}}} = - \frac{Y_1 m_1^{F0}}{(\Delta t_{\text{cycle}})^2} \left(1 - \frac{\partial t_{A1}}{\partial \Delta t_{\text{inj}}} \right) < 0 \quad (28)$$

For the average concentration of component 1 in product fraction A we derive Eq. (29). Again, for such large injection the plateau P1 prevails, $\partial t_{A1} / \partial \Delta t_{\text{inj}} = 0$ and the average concentration is constant. In the case of small injections, an increase in concentration is expected because $\partial t_{A1} / \partial \Delta t_{\text{inj}}$ was found to be a positive number in the parametric analysis.

$$\frac{\partial \bar{c}_1^A}{\partial \Delta t_{\text{inj}}} = \frac{\partial}{\partial \Delta t_{\text{inj}}} \left(\frac{Y_1 m_1^{F0}}{t_{A2} - t_{A1}} \right) = \frac{Y_1 m_1^{F0}}{(t_{A2} - t_{A1})^2} \frac{\partial t_{A1}}{\partial \Delta t_{\text{inj}}}$$

The average concentration of product fraction B, on the other hand, is always independent of injection width, as observed in Eq. (30).

$$\frac{\partial \bar{c}_2^B}{\partial \Delta t_{\text{inj}}} = \frac{\partial}{\partial \Delta t_{\text{inj}}} \left(\frac{Y_2 m_2^{F0}}{t_{B2} - t_{B1}} \right) = 0 \quad (30)$$

Finally, it should be noted that there exists a minimum injection width below which the design constraints (P , Y) cannot be matched exactly, but will be exceeded. In other words, for a sufficiently small injection, separation of the components becomes so good that, if the purity constraints are to be fulfilled for both product fractions simultaneously, there will be no recycle fraction. The minimum injection width is thus readily obtained from Eq. (4) by setting $t_{A2} = t_{B1}$, which yields

$$\Delta t_{\text{inj, min}} = \frac{\int_{\tau_{B1}}^{\tau_{B2}} c_2 dt}{c_2^{F0} Y_2} \quad (31)$$

The above findings can be summarized as follows:

- The throughput per cycle is independent of Δt_{inj} .
- The cycle and recycle times always increase with increasing Δt_{inj} .
- Correspondingly, the productivity PR always decreases with increasing Δt_{inj} .
- Eluent consumption EC decreases with increasing Δt_{inj} for small injections, but is independent of Δt_{inj} for large injections.
- Concentration of product fraction A increases with Δt_{inj} for small injections, but is independent of Δt_{inj} for large injections.
- Concentration of product fraction B is always independent of Δt_{inj} .
- Purity constraints can be matched exactly only above a certain minimum injection width relative to column length

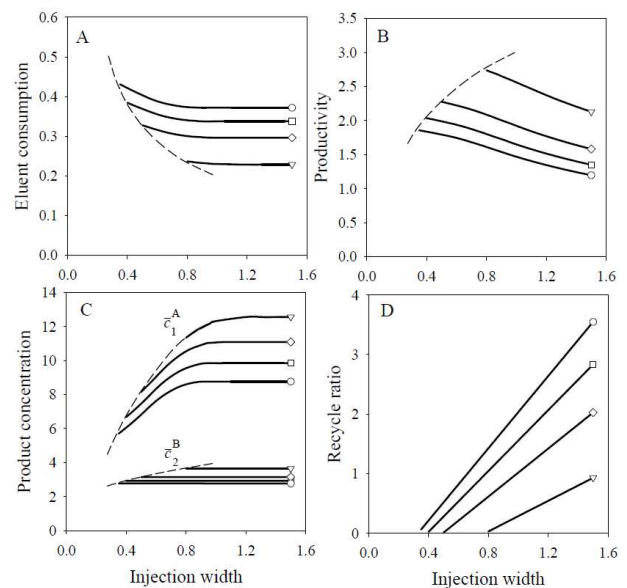


Figure 4. Effect of injection width Δt_{inj} on the performance of mixed-recycle SSR chromatography. Purity constraints ($P^A = P^B$): (∇) = 80%, (\diamond) = 90%, (\square) = 95%, (\circ) = 98%. Isotherm parameters and feed concentrations are given in the text.

Finally, it should be emphasized that these results are obtained by using dimensionless times (relative to the elution time of a non-retained compound) instead of real times, and the performance parameters are thus independent of the physical dimensions of the column.

4.2 Performance of the SSR process for a generic example

The calculation method presented above was applied to study the performance of mixed-recycle SSR chromatography for varying purity requirements of the product fractions. In view of the above findings, the effect of the operating parameter, Δt_{inj} , on PR , EC , and product concentrations was of particular interest. A generic example system was considered with a fresh feed concentrations of $c_1^{F0} = c_2^{F0} = 10 \text{ g L}^{-1}$. The parameters of the Langmuir isotherms, Eq. (9), were $q_{m,1} = q_{m,2} = 100 \text{ g L}^{-1}$, $b_1 = 0.02 \text{ L g}^{-1}$, and $b_2 = 0.025 \text{ L g}^{-1}$, respectively. The phase ratio, ϕ , was chosen equal to 1.5.

The dependence of the performance parameters on the injection width and purity constraints is displayed in Fig. 4. Eluent consumption and productivity are presented for component 1 only, since behavior for component 2 is similar. The dashed lines in the subfigures indicate the minimum injection width as determined from Eq. (31), below which the purity specifications cannot be matched exactly for both product fractions. In other words, the dashed lines represent the performance of batch chromatography operated in “stacked injections” mode with the same purity and yield constraints as the SSR process.

The eluent consumption (Fig. 4A) is found to be higher for higher purity requirements, and to decrease with increasing injection width until it levels off as the injection width becomes sufficiently large. The trend is therefore the same as predicted by Eq. (27). This result should be interpreted such an SSR process is always superior to batch chromatography in terms of eluent consumption.

Also the behavior of the productivity (Fig. 4B) is in accordance with the analysis presented above, see Eq. (28). The decrease in productivity with increasing Δt_{inj} can be explained also by considering that the recycle ratio, defined as $R = \Delta t_{rec} / (\Delta t_{inj} - \Delta t_{rec})$, increases rapidly as a function of injection width and increasing purity requirements (see Fig. 4D). A high recycle ratio obviously means a less efficient operation in terms of adsorbent usage since less fresh feed is introduced compared to the size of the recycle fraction. Batch chromatography has a recycle ratio of zero, and its productivity is always higher than that of SSR chromatography.

It is seen in Fig. 4C that using larger injections results in higher concentration of component 1 in product fraction A. The concentration of component 2 in product fraction B, however remains constant. These results are in accordance with Eqs. (29) and (30). With respect to the concentration of product fraction A, the SSR process always outperforms batch chromatography.

It is further observed in Fig. 4C that, just as in batch chromatography, also in mixed-recycle SSR processes the first eluted component can be obtained in higher concentration than in the fresh feed. This is the case for low purities and large injection widths only, however.

As usual in chromatographic separation, the optimum operating point is characterized by a trade-off between productivity, eluent consumption, and concentrations of the product fractions. It is interesting to note that, although lowering the purity constraints results in enhanced performance in terms of the considered performance parameters, it also narrows the range of feasible injection widths.

5. Applicability of the design method and operational aspects

5.1 Accelerated start-up and quality of prediction

An obvious question is how well applies the developed equilibrium-design approach to real chromatographic separations that always involve dispersive effects (due to mass-transfer resistances, axial dispersion, etc.). Furthermore, it should be clarified if the direct prediction of the steady state can be used to speed up the startup of the process. Below we will give an example that allows for a discussion of these two aspects.

Figure 5 shows steady state concentration profiles obtained from the equilibrium method for an injection width of $\Delta t_{inj} = 1$ and a desired purity of 98% for both fractions (dashed lines). The corresponding predicted cut times are $t_{A1} = 3.549$, $t_{A2} = 3.918$, $t_{B1} = 4.588$, and $t_{B2} = 5.75$, respectively; the feed concentrations in steady state are $c_1^F = 5.470$ and $c_2^F = 7.200$. The cut times were applied in dynamic cycle-to-cycle simulations using the equilibrium dispersive model (see, e.g., [21]), assuming a column with 1500 theoretical stages. Three different startup procedures were investigated. In the first option (Fig. 5, left) the process is started by the small injection fresh feed that is injected in each cycle (cf. Fig. 1, bottom). It can be observed that approximately 20 cycles are required to reach steady state during which performance improves slowly. The second option (middle of Fig. 5) applies initially a full injection of fresh feed (i.e., the injected volume corresponds to the sum of the volumes of recycle fraction and fresh feed). Steady state is obtained considerably faster (about 5 cycles). Although this option achieves better performance during startup, compared to the first option, during the first 5 cycles the purity of fraction A is off spec. In the third procedure (Fig. 5, right), the initial injection is performed using the predicted steady state feed concentrations (it is assumed that a corresponding mixture could be prepared for this first injection). Steady state is obtained basically with the third cycle and purity requirements are always fulfilled.

It is important to realize that all three scenarios lead to an identical steady state. Furthermore, a comparison with the concentration profiles predicted with the ideal model (dashed lines) shows a close agreement. However, in all cases, the limited column efficiency leads to lower product purities than the required 98% for both fractions (i.e., 97.0% is obtained for fraction A, and 94.5% for fraction B). Such deviations could be

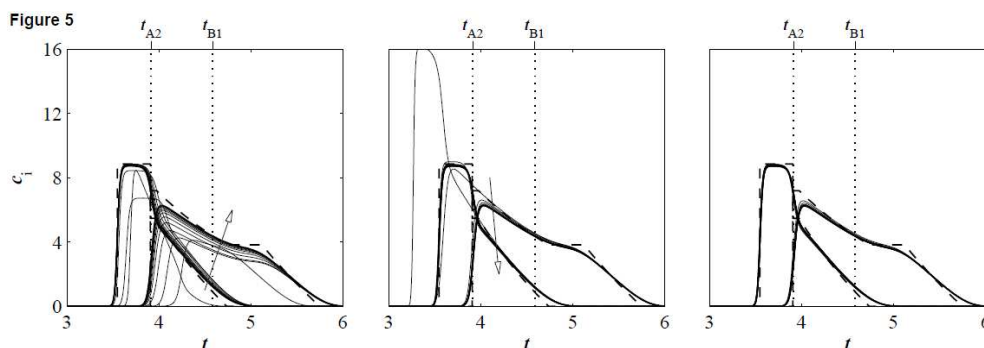


Figure 5. Transient behavior of mixed-recycle SSR processes. Startup procedures: small injection of fresh feed (left), full injection of fresh feed (middle), full injection of steady state concentrations predicted by design method (right). Solid line: calculated using an equilibrium dispersive model with 1500 theoretical stages. Dashed line: predicted steady state, calculated with the ideal model (Eq. (7)). In all three cases, identical design parameters were applied (see text). Thick line: cycle 25.

expected; they will be higher for systems where thermodynamic effects are less predominant (i.e., less efficient columns, smaller injection volumes and lower concentrations, respectively).

A viable option to rectify this mismatch could be to start the process according to Fig. 5 (right). Since steady state is obtained rapidly, product purities can be readily verified and cut times might be patiently adjusted. In this respect, the mixed-recycle SSR process is easier to operate than the closed-loop mode, which allows verifying the obtained purities only after attaining a steady state.

5.2 Operational Aspects

A short comparison of operational aspects of the mixed-recycle and the closed-loop SSR modes appears useful here, since the mixed-recycle mode seems to be largely neglected among practitioners. The main reason for this is the obvious loss of already achieved partial separation in this mode. However, in closed-loop mode, the recycle pump also causes significant back-mixing. Another important aspect is that in closed-loop SSR operation, the injection time point is coupled to the elution of the recycle. In contrast to this, in mixed-recycle mode these time points can be freely chosen and optimized such that the process operates in “stacked injections” mode (i.e., no gap exists between fraction B of the n -th cycle and fraction A of $(n+1)$ -th cycle). In fact, for long columns, even several elution profiles might pass simultaneously through the column. While a small safety gap is required in both modes to prevent overlaps of product fractions due to dispersion, the closed-loop mode requires additional regeneration time for the injection loop.

Despite the mentioned drawbacks of the closed-loop operation, an intriguing aspect of this mode is that the injection of the highly concentrated fresh feed can actually result in a beneficial change of the migration behavior of the components (for nonlinear isotherms). Model calculations indicate that, when using the cut times predicted with the above method in a closed-loop SSR process, higher purities of the first fraction can be obtained. This effect is related to non-linear interaction of the concentrations fronts. Similar effects are found in, for example, displacement chromatography (see [21]) or in advanced operating modes of Simulated Moving Bed processes [22]. More elaborated recycle modes as proposed in [7] introduce a similar

effect also in mixed-recycle mode. Further investigations of this aspect appear desirable.

Another aspect is related to a possible overlapping between consecutive cycles, which could be achieved in the mixed-recycle mode. For real systems, a small overlap might lead to shorter cycles. However, typically it is beneficial to only overlap low-concentrated parts of the bands that result from dispersion. This cannot be addressed using equilibrium theory. There, an overlapping shock front of the weak component would drastically decrease the purity of the “strong fraction”. More restrictive cut times would result that, in turn, constrict throughput (by larger recycle fractions or smaller injections). An analysis of this interesting, but difficult interplay is beyond the scope of this work.

Due to the specific advantages of the two operating modes, no general conclusion is possible which of the two modes will actually achieve better process performance. For a given system, both modes will have to be evaluated based on optimizations using appropriate models.

6. Conclusions

Analysis and optimal design of steady state recycling (SSR) chromatography in mixed-recycle operation were investigated in the framework of the equilibrium theory. A method was developed for direct prediction of the steady state and the relevant cut times corresponding to arbitrary purity or yield requirements for systems following the competitive Langmuir adsorption isotherm.

With this method, the steady state of the SSR process is obtained on the basis of adsorption isotherm parameters only, without requiring simulations using a dynamic column model. This greatly simplifies the design of SSR processes.

Theoretical analysis of SSR chromatography with mixed recycle revealed that the total injection width is the only free operating parameter since purity or yield specifications determine the cut times.

An intriguing finding is also that the achievable throughput per cycle is independent of total injection width, while the time periods for the whole cycle and the recycle increase linearly with this parameter. As a consequence, the productivity of such an SSR process is necessarily lower than that of an optimized separation by batch chromatography. On the other hand, the SSR process always outperforms batch chromatography in terms of eluent consumption and product concentrations.

The developed method also enables quantitative evaluation of process performance. The above theoretical findings were fully supported by results of a case study for a generic example system.

A brief discussion was given on the applicability of the equilibrium design approach to finite efficiency systems. Besides the expected deviations with respect to the ideal model, it could be demonstrated that using this design procedure allows to significantly shorten the startup time of the process, and thus to improve performance.

Further work appears interesting with respect to a detailed comparison between different operating modes for SSR chromatography, in particular since some of them entail an interesting dynamic behavior.

Acknowledgements

The authors gratefully acknowledge funding of this work by German Academic Exchange Service and the Academy of Finland. T. Sainio acknowledges financial support by Danisco Tutkimussäätiö s.r. and the LUT Research Foundation.

References

- 1 G. Subramanian (Ed.), *Chiral Separation Techniques - A Practical Approach*, Wiley-VCH, Weinheim, 2000.
- 2 K.J. Bombaugh, W.A. Dark, R.F. Levangie, *J. Chromatogr. Sci.* 7 (1969) 42.
- 3 Seidel-Morgenstern, G. Guiochon, *AIChE J.* 39 (1993) 809.
- 4 Heuer, A. Seidel-Morgenstern, P. Hugo, *Chem. Engng. Sci.* 50 (1995) 1115.
- 5 Duvdevani, J.A. Biesenberger, M. Tan, *Polym. Lett.* 9 (1971) 429.
- 6 M. Bailly, D. Tondeur, *Chem. Engng. Sci.* 37 (1982) 1199.
- 7 M. Bailly, D. Tondeur, *Chem. Eng. Process.* 18 (1984) 293.
- 8 D. Tondeur, M. Bailly, in: P. Barker, G. Ganetsos (Eds.), *Preparative and production-scale chromatography*, *Chromatographic Science Series*, v. 61, Marcel Dekker, New-York (1993) pp. 79-109.
- 9 F. Charton, *Optimisation des coupes et recyclages en chromatographie preparative industrielle*, PhD thesis, Institut National Polytechnique de Lorraine, Nancy, 1995.
- 10 F. Charton, M. Bailly, G. Guiochon, *J. Chromatogr. A* 687 (1994) 13.
- 11 C.M. Grill, *J. Chromatogr. A* 796 (1998) 101.
- 12 C.M. Grill, L. Miller, *J. Chromatogr. A* 827 (1998) 359.
- 13 C.M. Grill, L. Miller, T.Q. Yan, *J. Chromatogr. A* 1026 (2004) 101.
- 14 J. Kennedy, M. Belvo, V. Sharp, J. Williams, *J. Chromatogr. A* 1046 (2004) 55.
- 15 T.Q. Yan, C. Orihuela, *J. Chromatogr. A* 1156 (2007) 220.
- 16 M. Kaspereit, K. Gedicke, V. Zahn, A.W. Mahoney, A. Seidel-Morgenstern, *J. Chromatogr. A* 1092 (2005) 43.
- 17 M. Kaspereit, *Separation of enantiomers by a process combination of chromatography and crystallisation*, Shaker, Germany, 2006, pp. 98.
- 18 H.-K. Rhee, R. Aris, N.R. Amundson, *First-order Partial Differential Equations. Vol. I – Theory and Applications of Single Equations*, Dover, Englewood Cliffs, 2001.
- 19 H.-K. Rhee, R. Aris, N.R. Amundson, *First-order Partial Differential Equations. Vol. II – Theory and Applications of Hyperbolic Systems of Quasilinear Equations*, Dover, Englewood Cliffs, 2001.
- 20 F. Helfferich, G. Klein, *Multicomponent chromatography*, Marcel Dekker, New York, 1970.
- 21 G. Guiochon, D.G. Shirazi, A. Felinger, A.M. Katti, *Fundamentals of Preparative and Nonlinear Chromatography*, Academic Press, Boston, 2006.
- 22 H. Schramm, A. Kienle, M. Kaspereit, A. Seidel-Morgenstern, *Chem. Engng. Sci.* 58 (2003) 5217.
- 23 P.C. Wankat, *Rate-controlled separations*, Elsevier, New York, 1990.